Simple Frequency-Based Sensing of Viscosity and Dielectric Properties of a Liquid Using Acoustic Resonators

Diethelm Johannsmann,[1] *Wendelin Bücking,*[1] *Berthold Bode,*[2] *Judith Petri*[1]

[1]Institute of Physical Chemistry, Clausthal University of Technology, Arnold-Sommerfeld-Str. 4, 38678 Clausthal-Zellerfeld, Germany
[2] Flucon fluid Control GmbH, Burgstätterstr. 6, D-38678 Clausthal-Zellerfeld, Germany

ABSTRACT

The effects of a finite polarizability of a liquid sample onto the series resonance frequency of a piezoelectric resonator are described within the small-load approximation. It is found that the sample's electrical capacitance (the ratio of surface potential and surface polarization at the crystal surface) enters the motional branch of the equivalent circuit, thereby shifting the series resonance frequency. This effect comes about by piezoelectric stiffening. Using a conventional quartz crystal with small hole in the front electrode and exposing this crystal to a variety of different liquids, we demonstrate that derived equation describes the experiment reasonably well.

Electric and dielectric effects are particularly strong for torsional resonators, which operate at a frequency of around 56 kHz. These are in commercial use for determination of the viscosity of engine oils. We propose a simple method to in-situ switch the strength of piezoelectric stiffening. The technique is based on a pair of wires around the crystal, which – if connected to each other – shield the environment from the electric field emanating from the crystal. Closing the switch therefore reduces the overall energy the strain-induced electric field, which reduces the effective stiffness of the crystal and, in consequence, the resonance frequency. This simple device allows to separate the viscoelastic parameters from the polarizability. It could, for instance, be used to differentiate between gasoline and water being accidentally admitted to the lubricant reservoir. The instrument requires a single resonator and is based on the determination of two frequency shifts, only.

I. INTRODUCTION

Effects of finite conductivity and dielectric permeability are well known to influence the outcome of sensing employing piezoelectric devices such as the quartz crystal microbalance (QCM)[1] or surface acoustic wave (SAW) sensors.[2] The influence of the electrical potential at the surface is twofold. Firstly, it affects the parallel capacitance of the device, C_0. This effect is of some relevance and has been put to use in order to probe the polarity of the liquid

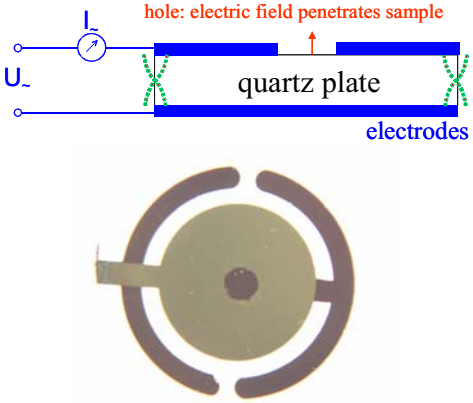

Fig. 1: If there is a small hole in the front electrode, the pattern of motion will not be changed appreciably by the presence of the hole. However, the surface polarization induced by piezoelectricity will radiate an electric field into the sample, thereby changing the series resonant frequency. The effect is based on piezoelectric stiffening. Top: Schematic view. Bottom: Optical micrograph of a 1-inch quartz crystal containing a hole (3 mm diameter) in the front electrode. The hole appears dark because it exposes the chromium adhesion layer of the back electrode. The data shown in Fig. 4C were taken with this resonator.

under study a long time ago.[3] There is a second class of effects, which has to do with piezoelectric stiffening.[4] The stiffness of a piezoelectric material depends on whether or not the electrodes are short-circuited.[5] In case they are not, there is an electric contribution to overall strain energy of the crystal. The field emanating from the crystal contributes to the total strain energy with about 0.7% for AT-cut quartz crystals, thereby contributing the crystal's effective stiffness. Should, on the contrary, the electrodes be electrically short-circuited, the external charge compensates the surface polarization and the strain energy is of entirely elastic origin. Piezoelectric stiffening is well-known in the frequency control community, because it can be used to "pull" the frequency of an oscillator with an external capacitor.[6] Even though the electric contribution to the total energy is small, piezo-electric stiffening may be very significant in terms of the frequency shift (~10 kHz). Importantly, piezoelectric stiffening affects the motional branch of the equivalent

978-1-4244-3510-4/09/$25.00 ©2009 IEEE

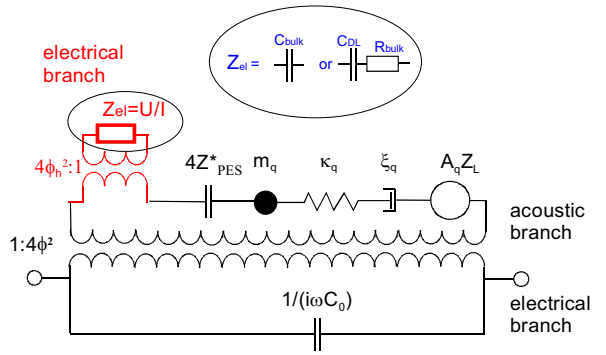

Fig. 2: Equivalent circuit explicitly describing the influence of the *electric* impedance of an open crystal surface onto the resonance parameters. The electric impedance is the ratio of the surface potential (relative to the electrode next to it) and the electric current (that is, the time derivative of the surface polarization). C_0 is the parallel capacitance, m_q is the effective mass of the crystal, κ_q is the effective spring constant, ξ_q is the effective drag coefficient, A_q is the effective area, Z_L is the load impedance, Z^*_{PES} covers piezoelectric stiffening for the portion of crystal covered by electrodes, and the parameter ϕ converts between acoustic and electrical quantities. Inset: The electrical may impedance may either be a simple capacitor (dielectric medium) or a capacitor representing the electric double layer and a resistor representing the bulk (conductive salt solution). More complicated circuits are possible as well, for instance, if electrochemical reactions occur at the electrode surface.

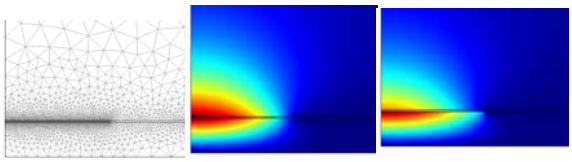

Fig. 3: Finite element calculations of the average surface potential $\langle U \rangle_h$ to be entered into Eq. 3. The calculation makes use of the electrostatics module of the software package COMSOL. The geometry is 3D with axial symmetry, where the axis of symmetry (the center of the crystal) is to the left. Top: Geometry and mesh. The central hole in the electrodes is covered with an electric double layer. For the purpose of simulation, the film has been made unrealistically thick and the dielectric permittivity has been decreased in proportion. Center: distribution of electrical potential in pure water. Bottom: Distribution of electrical potential in water containing 1 mol/L NaCl. The electric double layer screens the electric field. The quantity $\langle U \rangle_h$ is obtained in the post-processing mode by integrating the voltage over the hole.

circuit and therefore shifts the series resonance frequency, f_s. As opposed to the parallel capacitance, C_0, the series resonance frequency can be easily measured with a precision in the range of 10^{-7}. Electric and dielectric properties of the sample are therefore conveniently probed via electro-acoustic coupling.

Many workers would view electrical interactions between the crystal and its environment as a source of artifacts. In order to stay away from such problems, grounding the front electrode is always advised. π-networks are employed for a similar purpose.[7] A π-network is an arrangement of resistors, which almost short-circuit the two electrodes. This makes the device less susceptible to electrical perturbations. Evidently, short-circuiting must be incomplete, because the resonator would otherwise be electrically separated from the testing equipment. However, electrically opening the front surface to the environment can also be an interesting option because it allows sensing the electrical properties of the sample.[3] The fact itself has been described before.[3,8] It has recently seen revived interest in the context of the lateral field excited (LFE) resonator.[9,10,11,12,13]

This contribution is concerned with two developments. In the first part, we describe how polarization effects can be described in the frame of the small-load approximation.[14,15] In the second part, we show how polarization effects can be put to work in a very simple way to separately probe the viscoelastic properties and the polarizability of a liquid medium. The instrument needs a torsional resonator, a pair of wires, and a simple switch.

II. Electrid Field Induced-Frequency Shifts as Derived within the Small Load-Approximation

Before embarking on the description of polarization effects in the frame of the small load-approximation,[16] we would like to point out that EerNisse and co-workers have carried out a detailed finite element method (FEM) calculation of the same problem.[17] These calculations are a benchmark. They are much more accurate than the treatment below. However, they are demanding as well. The treatment proposed below leads to simple equations, which can be applied by anyone. For the more mathematically inclined researcher, there is a numerical type of analysis building on the small load approximation, which requires FEM software but still is much simpler than the FEM calculations from Ref. 17.

For the laterally homogeneous plate, piezoelectric stiffening is accounted for by a negative capacitance in the BvD circuit.[4,18] For the electrode-covered plate, the magnitude of this element is

$$Z_{PES} = -4\phi^2 \frac{U}{I} = -4\phi^2 \frac{1}{i\omega C_0} = -4\left(\frac{A_q e_{26}}{d_q}\right)^2 \frac{1}{i\omega C_0} \qquad \text{Eq. 1}$$

where the parameter $\phi = A_q e_{26}/d_q$ translates between mechanical impedances (in units of force/speed) and electrical impedances (in units of voltage/current). $C_0 = A_q \varepsilon\varepsilon_0/d_q$ is the electrical ("parallel") capacitance between the electrodes. A_q is the active area of the crystal, e_{26} is the piezoelectric stress coefficient, and d_q is the thickness.

Importantly, the value of Z_{PES} differs from Eq. 1 if part of the active region is not covered by the electrode. Consider the geometry depicted in Fig. 1, where the front electrode contains a central hole. Inside the hole, the surface polarization is uncompensated, which generates an excess electric field both inside the crystal and in the adjacent sample. The excess electric field creates a mechanical stress, which leads to an increase in frequency. Should the sample,

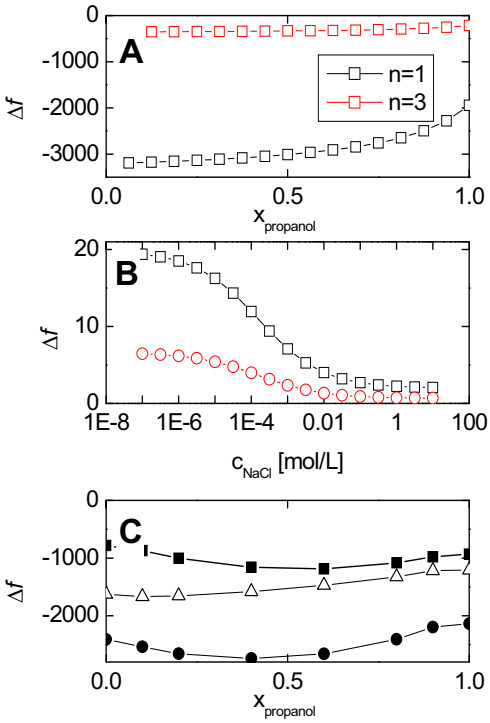

Fig. 4: A: Frequency shift calculated for a mixture of propanol and water. The radius of the central hole is 1.5 mm. The dielectric constant of the medium was approximated as $\varepsilon \sim 80\text{–}70\ x_{propanol}$. Only the polarization contribution is shown, the variability of Δf related to a change of viscosity with propanol content is ignored. The data were obtained by calculating the mean surface potential inside the hole with an FEM simulation and inserting the ratio of $\langle U \rangle_h$ and surface polarization into the small load approximation (Eq. 3). B: Similar calculation, where the sample was water with variable concentration of NaCl. The salt affects both the bulk conductivity and the double layer capacitance. C: Experimental frequency shifts at the fundamental in a mixture of the water and propanol. Full squares: conventional crystal with no hole. Full dots: crystal with central hole as shown in Fig. 1. Open triangles: difference between the two.

however, be polarizable, the piezoelectric polarization at the crystal surface will be partly compensated by the induced polarization in the sample, thereby decreasing the field energy and the resonance frequency.

A shear-induced electric polarization of the sample can be described as a load in essentially the same way as this is usually done for mechanical loads. An accordingly expanded equivalent circuit is shown in Fig. 2. The motion of the crystal couples to an *electrical* impedance (U/I) at the crystal surface. The coupling coefficient, ϕ_h, is different from ϕ in Eq. 1 because the relevant area is the area of the hole, A_h, (rather than the area of the crystal, A_q). The element accounting for piezoelectric stiffening was split in a first part, Z^*_{PES}, covering the remaining (electrode-covered) portion of the crystal and a second part, Z_h, describing the open part. This second element is given by

$$Z_h \approx 4\phi_h^2 \frac{\langle U \rangle_h}{I} \approx \frac{4e_{26}^2}{d_q^2} \frac{A_h \langle U \rangle_h}{i\omega\sigma_S} \qquad \text{Eq. 2}$$

The second relation makes use of $I = i\omega A_h \sigma_S$ with σ_S the surface polarization. In the spirit of the small load approximation,[19] the potential difference between the crystal surface and the neighboring electrode, U, was replaced by its average, $\langle U \rangle_h$. The average is taken over the area of the hole.

When $\langle U \rangle_h$ shifts due to the presence of the sample, the corresponding frequency shift is calculated as:

$$\frac{\Delta f_{PES}^*}{f_F} = \frac{i}{\pi Z_q} \frac{\Delta Z_h}{A_q} = \frac{i}{\pi Z_q A_q} 4\phi_h^2 \frac{\langle \Delta U \rangle_h}{i\omega\sigma_S} = \frac{i}{\pi Z_q A_q} 4\phi_h^2 \frac{\langle \Delta U \rangle_h}{I} \qquad \text{Eq. 3}$$

f_F is the frequency of the fundamental and Z_q is the acoustic impedance of AT-cut quartz. An index PES was added to the frequency shift in order to emphasize that eq. 3 only covers effects due polarizability. Effects of viscosity and/or mass loading have to subtracted. This could be done by preparing an analogous sample on a crystal with no hole and subtraction the frequency shifts obtained on the two devices.

Eq. 3 connects a frequency shift to an electrical impedance, which is a ratio of voltage and current. It is written in a form emphasizing the analogy to the small load approximation, where the latter states that the frequency shift is proportional the ratio of stress and speed at the crystal surface. Note that Eq. 3 is complex. The real part of Δf^* is the conventional frequency shift. The imaginary part is the change in the half bandwidth at half maximum. The term on the right-hand-side is complex because there may be a phase shift between the voltage and the current.

If the sample is a simple dielectric medium, the sample may be represented as a simple capacitor. Its value is proportional to the sample's dielectric permittivity, ε. The permittivity can therefore be measured in this way. More specifically, one has:

$$\frac{\Delta f^*}{f_F} = \frac{i}{\pi Z_q A_q} 4\phi_h^2 \frac{1}{i\omega C} = \frac{1}{\pi Z_q A_q} 4\phi_h^2 \frac{\alpha}{i\omega\varepsilon_0} \frac{1}{\varepsilon} \qquad \text{Eq. 4}$$

C is the capacitance constituted by the hole and the neighboring electrode. α is a geometrical factor with units of a length. For a conventional capacitor, α would be the ratio of area and thickness. Eq. 4 shows that Δf is proportional to the inverse dielectric constant.

In an electrochemical environment, the sample may have to represented by a more complicated circuit than a simple capacitor. For instance, the Randles circuit needs three elements, which are the charge transfer resistance, R_{CT}, the resistance of bulk, R_{bulk}, and the double layer capacitance, C_{DL}. In a way, inferring the electrical surface impedance from frequency shifts amounts to a type of electrochemical impedance spectroscopy (EIS).[20] Note, however, that conventional EIS instrumentation works at frequencies below 1 MHz, whereas the QCM operates at many MHz. Also, the frequency range of the QCM is limited to less than

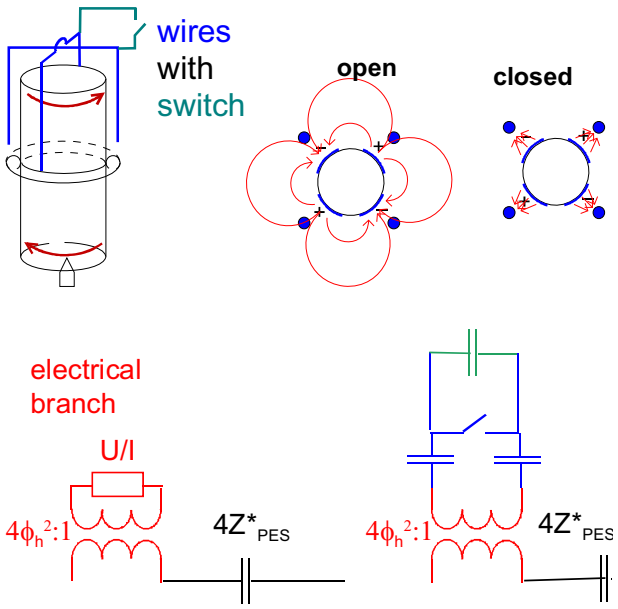

Fig. 5: Sample geometry for partial screening of the electric field emanating from a torsional resonator be means of a set of external U-shaped wires. The electric field is short-circuited, if the two parts wires are electrical connected (top right). By opening the switch, one increases the electric contribution to the strain energy and the effective stiffness of the crystal (top center). The bottom part shows the portion of the equivalent circuit dealing with piezoelectric stiffening. Part of the sample's capacitance can be short-circuited with the switch.

a decade. Still, this type of measurement is conceptually equivalent to QCM-based EIS.

In order to predict the area-averaged surface potential (given a certain strain-induced surface polarization, dictated by the driving amplitude of the crystal) one will presumably have to resort to finite element modeling in most cases. This model is rather simple. It only has to cover the electric properties (possibly the electrochemical properties) of the sample near the hole. The resonator as such remains outside of the calculation. That is the central virtue of the small load approximation. Making use of the small-load approximation, one may confine modeling to the determination of a surface impedance (be it a stress-speed ratio or a voltage current ratio).

Fig. 3 shows the raw output of such an FEM calculation. The geometry and the mesh are displayed at the top. The crystal is modeled as an isotropic dielectric. The geometry is three-dimensional, but there is an axis of rotational symmetry (to the left in Fig. 3). The crystal extends much further to the right than what is displayed in Fig. 3. The radius of the crystal is 1 cm. The bare hole in the center of the crystal (to left in Fig. 3) has a radius of 1.5 mm and a surface charge of $\sigma_S = 1$ C/m^2. The value of the surface charge does not matter since the average surface potential, $\langle U \rangle_h$, is proportional to the surface charge. Only the ratio of the two enters Eq. 3. The electrodes and the other boundaries of the cell are grounded. Above, the hole is a

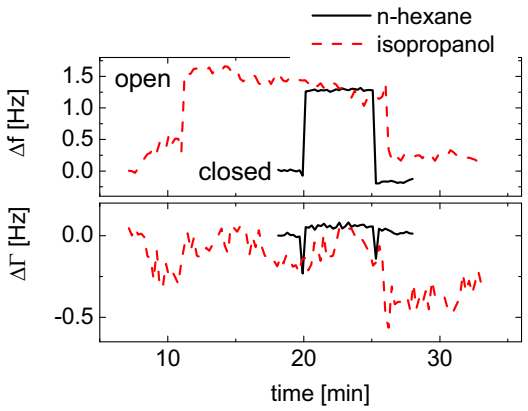

Fig. 6: Shifts of frequency (Δf) and bandwidth ($\Delta\Gamma$) induced by switching the state of the wiring in *n*-hexane in isopropanol. The change is larger in n-hexane because this liquid has the smaller dielectric constant.

planar layer with a thickness of 50 µm. This layer emulates an electric double layer. The thickness has to be chosen unrealistically large in order to accommodate a mesh with reasonably large spacing. In order to compensate for related artifacts, the layer's dielectric constant, ε, is decreased accordingly. By this computational trick, the capacitance (proportional do ε/d with d the thickness) *is* realistic and the electric properties of the entire ensemble are well represented. All dielectric constants may be complex. For instance ε" is given by $\sigma/(\omega\varepsilon_0)$ if the material has some finite conductivity, σ. The center and the bottom panel show the electrical potential distribution for pure water and for a solution of a 1-1 electrolyte like NaCl. In the latter case, the electric double layer screens the electric field.

Fig. 4 shows the derived frequency shifts on the fundamental and on the third harmonic for a water / propanol mixture (top) and an aqueous salt solution (bottom). Panel A is intended to qualitatively reproduce the experiments shown in Fig. 4 of Ref. 11. The frequency increases with increasing propanol content because propanol is less polarizable than water. The dielectric constant was approximated as $\varepsilon \sim 80 - 70\, x_{\text{propanol}}$. In Ref. 11, the overall increase in frequency is in the kHz range, whereas it is a few hundred Hertz, here. The difference goes back to the fact that a small hole in the front electrode was employed in the calculation, whereas the entire front surface was exposed the liquid in Ref. 11. Panel C shows an experiment from our own group, undertaken with the crystal shown in Fig. 1. The full and the dotted line show Δf obtained with and without a hole, respectively. For the crystal containing a hole, Δf varies because of variable viscosity as well as variable dielectric constant. Subtracting the values obtained with the conventional quartz (which responds to viscosity, only) yields the effects due to variable ε (open squares). The open squares in Panel C are to be compared to the open squares in panel A. In both cases Δf increases with propanol content. The order of magnitude (a few hundred Hz) is the same in theory and experiment.

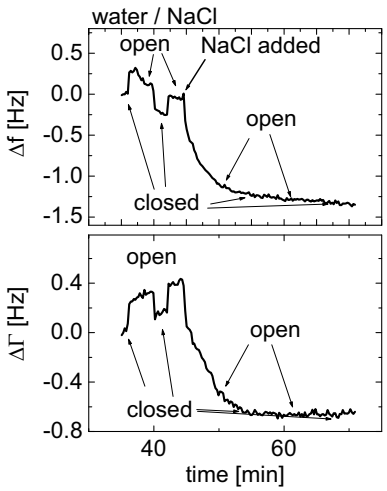

Fig. 7: Shifts of frequency (Δf) and bandwidth ($\Delta\Gamma$) induced by switching the state of the wiring in water. When salt is added, an electric double layer develops at the crystal surface, which completely screens the crystal from the external circuitry. Note that the liquid in this case should not be modeled as a simple capacitor, but rather as a capacitor (representing the electric double layer) in series with a resistor, quantifying the liquid's finite bulk conductivity.

Since the agreement is not quantitative the instrument needs calibration with liquids of known dielectric constant.

Panel B in Fig. 4 is intended to reproduce the experiment shown in Fig. 16 of Ref. 9. Again the frequency decreases with increasing salt concentration due to the electric double layer. However, the magnitudes of the effects are vastly different. The effect amounts to 10 Hz here, whereas it is 15 kHz in Ref. 9. Such a difference cannot be explained by the size of the hole, alone. The reason for this discrepancy at this point is not entirely clear. Possibly, it has to do with a change of the mode shape induced by presence of the electrolyte.

III. Separate Sensing of Viscosity and Polarizabilityx of a Liquid Based on Torsional Resonators and an External Conductor

Below, we describe a piezoelectric device which can be switched from one state, where the effects of polarizability are strong, to a second state, where they are weak. Comparing the frequency shifts obtained in these two states, one may separate the effects of viscosity and polarizability. Looking into the details, it turns out that such a two-state situation can be very easily accomplished for torsional resonators. For these devices, the effects of polarizability are considerably stronger than for thickness-shear resonators. Since torsional resonators actually are in commercial use as viscosity sensors to a larger extent than thickness shear resonators, we employed these for demonstrating the two-state device.

Torsional resonators are known from the beginning of research on piezoelectric resonators.[21,22] They have mostly been used to determine the viscosity of complex media at high frequencies.[23,24,25,26,27,28,29] We have recently provided a detailed description of the resonators used in the study reported here.[30] The resonators are marketed by Flucon fluid control GmbH. They are composed of rods of x-cut quartz with a length of 35 mm and a diameter of 12 mm. The units employed here are mounted with a pin at the center of one of the faces and an O-ring around the waist (Fig. 5). Only the upper portion of the resonator is exposed to the liquid. The lower portion carries the electrodes (in quadrupolar arrangement, right-hand-side in Fig. 5) and is sealed from the sample via the O-ring. Since the upper portion of the crystal does not carry electrodes, this device is strongly susceptible to effects of finite polarizability

In order to see that the effects of polarizability actually are stronger at lower frequencies, consider the following form of the small load approximation:[30]

$$\Delta f^* = \frac{1}{2\pi\, M_{Res}} \int_{Surface} w(r)\, Z_L(r)\, \mathrm{d}A \qquad \text{Eq. 4}$$

M_{Res} is the mass of the resonator, dA is an infinitesimal surface element, $w(r)$ is a statistical weight proportional to the square of the local amplitude of oscillation and $Z_L(r)$ is the load at position r. The usual form of the small load approximation ($\Delta f^*/f_F = \mathrm{i}/\pi\ Z_L/Z_q$) is recovered by realizing that for a thickness shear resonator, the mass is given by $A_q Z_q/(2f_F)$ and by approximating $w(r)$ as unity. Eq. 4 applies to both thickness shear resonators and torsional resonators.

We intend to compare the effects of viscosity to the effects of polarizability. For this comparison, all geometric factors contained in Eq. 4 are unessential. It suffices to compare the loads. For a Newtonian liquid, the load is $Z_L = (\mathrm{i}\rho\omega\eta)^{1/2}$, it scales as $\omega^{1/2}$. The dielectric load, on the other hand, scales as ω^{-1} (assuming that the electric load is mostly capacitive, $Z \sim 1/(\mathrm{i}\omega C)$). The ratio of the two therefore scales as $\omega^{-3/2}$. Effects of polarizability are much more severe at low frequencies. In fact, they are the limiting factor for the determination of viscosity in aqueous solutions with torsional resonators. Conversely, if polarizability and viscosity are both to be monitored, torsional resonators are the instruments of choice. Their frequency is about a factor of 100 lower than the frequency of the standard thickness shear devices.

Fig. 5 shows the geometry. A pair of U-shaped wires is placed such that they surround the active portion of the crystal. They were positioned opposite to the electrodes (where the latter are arranged in quadrupolar geometry). Connecting the two wires puts them to the same potential. The electric field then is mainly concentrated between the electrodes and the external wires and the electric field energy decreases accordingly (top right in Fig. 5).

Fig. 6 shows an experimental example. The jumps in frequency occurred when the switch was opened and closed.

For *n*-hexane and isopropanol, the effect amounts to a frequency shift of the order of 1 Hz. The effect is a bit stronger for *n*-hexane, reflecting the fact that n-hexane as a slightly smaller polarizability.

Fig. 7 shows corresponding data for water. Interestingly, there is a significant change of bandwidth connected to opening and closing the switch. Clearly, the situation is more complicated than for n-hexane. Presumably, this has to do with the fact that water is conductive and will develop an electric double layer at the crystal surface. The liquid cannot be modeled as a simple capacitor, an equivalent circuit must at least contain a capacitor and resistor on series, where the capacitor would represent the double layer and the resistor would represent the conductive bulk liquid.[31,32] As expected, switching has no effect onto the resonance frequency, once salt has been added in large amounts. Added salt increases the double layer capacity, leading to a situation where the crystal surface does no longer interact with the external circuitry.

The strain-induced surface potential may easily reach tens of volts. Such a high potential will not usually lead to electrochemical processes because the voltage drop occurs between the crystal surface and the nearby electrode, while electrochemical processes are driven by the potential drop right at the surface. As long as most of the voltage across the electric double layer is small (which is the case hat high frequencies), electrochemistry should not be a concern.

In principle, a similar type of switch should also be possible for high-frequency thickness-shear resonators. Our attempts to implement such a configuration proved difficult because the external wires acted as antennae and the derived frequency shift depended strongly on the exact position of the wires (cf. Fig. 7 in Ref. 11). Presumable, such a switch must be realized with additional electrodes evaporated onto the top surface of the crystal.

IV. Conclusions

Effects of finite polarizability can be straight-forwardly described in the frame of the small load approximation. The complex frequency shift is proportional to the area-averaged voltage/current ratio at the crystal surface. Experiments with a QCM, the front electrode of which contained a small hole confirmed this prediction reasonably well. Effects of finite polarizability are particularly strong for torsional resonators due to their low frequency. For strong effects of polarizability, one may actually switch the strength of the effect with external circuitry. Depending on whether or not the external wires provide some shielding, the effects of liquid polarizability are large or small. Using this simple device allows for frequency-based sensing of both viscosity and polarizability with a single resonator.

V. References

1 C. Steinem, A. Janshoff (edts.), *Piezoelectric Sensors*, Springer 2006.
2 F. Martin, M.I. Newton, G. McHale, Ka.A. Melzak, E. Gizeli, *Biosensors and Bioelectr.* **19,** 627 (2004).
3 Z.A. Shana, F. Josse, *Anal. Chem.* **66**, 1955 (1994).
4 R.N. Thurston, in C. Truesdell (edt.) *Mechanics of Solids*, vol. 4, chap. 36, p. 257, Springer, Heidelberg 1984.
5 W.G. Cady, *Piezoelectricity*, McGraw Hill, New York 1946.
6 P. Horowitz, W. Hill, *The Art of Electronics*, 2nd ed., Cambridge University Press, New York, 1989.
7 IEC standard 60444-1.
8 Z. A. Shana, H. Zong, F. Josse, D. C. Jeutter, *J. Electroanal. Chem.* **379**, 21 (1994).
9 U. Hempel, R. Lucklum, P. R. Hauptmann, E. P. EerNisse, D. Puccio, R. F. Diaz, *Meas. Sci. Technol.* **19**, 055201 (2008).
10 E. Hatch, A. Ballato *IEEE Ultrason. Symp. Proc.* **1**, 512 (1983).
11 U. Hempel, R. Lucklum, J. F. Vetelino, P. Hauptmann, *Sensors and Actuators A* **142**, 97 (2008).
12 Y. H. Hu, L. A. French, K. Radecsky, M. P. da Cunha, P. Millard, J. F. Vetelino, *IEEE Transactions on Ultrasonics, Ferroelectrics and Frequency Control* **11**, 1373 (2004).
13 C. Zhang, J. F. Vetelino, *Sensors and Actuators* **B 91**, 320 (2003)
14 F. Eggers, Th. Funck, *J. Phys. E: Sci. Instrum.* **20**, 523 (1987).
15 D. Johannsmann, K. Mathauer, G. Wegner, W. Knoll, *Phys. Rev. B* **46**, 7808 (1992).
16 The small load approximation also carries the name „surface impedance concept". See, for instance: H.L. Bandey, S.J. Martin, R.W. Cernosek, A. R. Hillman, *Anal. Chem*. **71**, 2205 (1999), R. Lucklum, C. Behling, P. Hauptmann, *Anal. Chem.* **71**, 2488 (1999).
17 E.P. EerNisse, D. Puccio, R. Lucklum, U. Hempel, *Frequency Control Symposium, 2008 IEEE International Volume* **19-21**, 31 (2008)
18 The negative capacitance is sometimes lumped into the motional capacitance, C_1. The latter then acquires a small dependence on overtone order. See, for example: A. Arnau ed., *Piezoelectric Transducers and Applications*, Springer 2004.
19 D. Johannsmann, *Physical Chemistry Chemical Physics* **10**, 4516 (2008).
20 A good tutorial on EIS is found at www.gamry.com/App_Notes/EIS_Primer/EIS_Primer. htm
21 W.P. Mason, *Piezoelectric Crystals and their Applications to Ultrasonics*, Van Nostrand, Princeton 1948.
22 H.J. McSkimin, *J. Acoustical Society of America* **24**, 117 (1952).
23 T. M. Stokich, D. R. Radtke, C. C. White, J. L. Schrag, *J .Rheology* **38**, 1195 (1994).
24 L. Kirschenmann, W. Pechhold, *Rheologica Acta* **41**, 362 (2002).
25 G. Fritz, W. Pechhold, N. Willenbacher, N. J. Wagner, *J .Rheology* **47**, 303 (2003).
26 T. Nakken, G. H. Nyland, K. D. Knudsen, A. Mikkelsen, A. Elgsaeter, *J. Non-Newtonian Fluid Mechanics* **52**, 217 (1994).
27 M. Eugster, K. Hausler, W. H. Reinhart, *Clinical Hemorheology and Microcirculation* **36**, 195 (2007).
28 D. Valtorta, E. Mazza, *Rheologica Acta* **45**, 677 (2006).
29 B. Bode, PhD thesis, Clausthal University of Technology 1984.
30 W. Bücking, B. Du, A. Turshatov, A.M. König, I. Reviakine, B. Bode, D. Johannsmann, *Rev. Sci. Instr.* **78**, 074903 (2007).
31 H.L. Girault, *Analytical and Physical Electrochemistry*, EPFL Press 2004.
32 R. Etchenique, T. Buhse, *Analyst* **127**, 1347 (2002).